A test of piezoelectricity in the chloride at the temperature of liquid nitrogen with an apparatus similar to that designed by Stokes (1947) was negative. However, no conclusion could be drawn, since either the piezoelectric effect might be too slight to detect, or the piezoelectric effects of many small domains might not be detectable in our apparatus. A chloride crystal remained dark when viewed between crossed polaroids along the *c* axis as the temperature was lowered through the transition interval. Since the low-temperature structure is definitely monoclinic, one may conclude either than the change in optical properties is slight, or that the domains are submicroscopic in size.

### References

HUGHES, E. W. & LIPSCOMBE, W. N. (1946). *J. Amer. Chem. Soc.* **68**, 1970.
KAY, H. F. (1948). *Acta Cryst.* **1**, 229.
KING, M. V. & LIPSCOMB, W. N. (1950). *Acta Cryst.* **3**, 222.
STOKES, R. G. (1947). *Amer. Min.* **32**, 670.

*Acta Cryst.* (1950). **3**, 230

# Deficiencies in Order of Large Size in Fibrous Systems†

BY RICHARD S. BEAR AND ORVIL E. A. BOLDUAN‡

*Department of Biology, Massachusetts Institute of Technology, Cambridge, Massachusetts, U.S.A.*

(*Received* 19 *April* 1949 *and in revised form* 3 *November* 1949)

A number of the fibrous proteins show small-angle diffraction of X-rays lacking evidence of the full complement of lattice translations characterizing normal crystalline order. Criteria for the judgment of the number of ordered dimensions from diffraction phenomena are particularly simple at small angles and are derived herein. These involve examination of diffraction shapes and the displacement of diffractions with tilting of the fibrous specimen from the normal perpendicular relationship to the incident beam.

Simple geometrical considerations suffice to show qualitatively the properties of the disk- or rod-like shapes characterizing diffracting arrays or nets in reciprocal space. These diffractors are usually conceived as of unlimited extension along ordered dimensions, but very thin transverse thereto. In practical cases the properties of the reciprocal-space disks and rods account for the diffraction broadening caused by reduction in particle dimensions along axes of order, or the sharpening effect of increased size along non-ordered directions—factors which complicate the simple criteria mentioned above. While disk or rod dimensions are normally independent of diffraction indices, this does not hold when the diffractors are internally distorted.

## Introduction

Certain protein fibers which have been investigated by means of small-angle X-ray diffraction (Bear, 1944*a*, *b*, 1945) and electron microscopy (Schmitt, Hall & Jakus, 1942; Hall, Jakus & Schmitt, 1945) showed evidence of periodic structure along only one (collagen) or two (paramyosin) fibril dimensions. These results gave rise to the question as to whether the remaining dimensions in each case did not, in fact, possess long-range order or whether the experimental evidence was deficient. The present paper considers the problem of obtaining definitive evidence for the number of dimensions possessing order, as independently as possible of a failure of intensity in the diffractions necessary for demonstration of order along a doubtful fibril direction.

Systems possessing one- and two-dimensional order are well known (cf. the linear arrays of halogen atoms described by West (1947) and the planar nets of carbon black discussed by Warren (1941) and by Biscoe & Warren (1942)). Indeed, Nowacki (1946) has attempted a rough classification, according to the number of axes of order, for substances yielding discontinuous small-angle diffraction. It has also been understood for some time that diffracting arrays and nets possess shape transforms resulting in disk- or rod-like distributions of intensity about each peak in reciprocal space (see Ewald, 1940). These concepts have not often been required, however, so that most accounts are concerned with the results of the application of the reciprocal lattice to three-dimensional crystals.

Reduction in the number of axes of order is not the only type of order-deficiency that may be encountered in fibrous systems. James (1948), in particular, noted some of these, emphasizing the importance of the diffraction aspects of thin linear arrays or limited imperfect aggregates of these in the study of fibers. Diffraction shapes are influenced by the degree of extension in space of both ordered and non-ordered

† This paper represents a partial report on research sponsored by the Office of the Quartermaster General, Research and Development Branch, under Project no. 130–46 on 'Determination of the Nature and Properties of Skin Structure', under direction of the Leather Subcommittee of the National Research Council Committee on Quartermaster Problems.

‡ Present address: Camp Detrick, Frederick, Maryland, U.S.A.

dimensions of the diffractor, as well as by internal distortions of the structure. Consequently, in deriving criteria for the systematic determination of axes of order, as is done below, it is necessary to keep in mind these additional factors.

The discussion starts with the case of a linear array of equivalent nodes, developing therefrom examples with higher order. Because the results are to be applied to protein fibers, certain conventions may be adopted at the outset: inspection of the known facts regarding small-angle diffraction by these systems discloses that the bulk fiber axis can probably always be considered as paralleling one lattice axis of each of the individual ultra-microscopic diffracting elements (fibrils), and that this axis is nearly orthogonal to other transverse structural axes, since prominent diffraction row lines are alway approximately normal to layer lines on the fiber patterns. Consequently, for the present purposes it is sufficient to employ with three-dimensionally ordered fibrils the conventional monoclinic elements $a_0$, $b_0$, $c_0$ and $\beta$ for unit-cell description. It is convenient to discard $c_0$ and $\beta$ for two-dimensional cases, and in addition $a_0$ may be dropped for one-dimensional systems. In all cases $b_0$ remains the structure period along the fibril axis.

### Representation of one-dimensional order in reciprocal space

Fig. 1 shows a linear array of nodes extending along $Cy$. An incident X-ray beam arriving in the direction $AC$ continues toward $O$. It also gives rise to diffracted beams, one of which is shown directed toward $P$. In the figure the angles of incidence and of diffraction, $\theta$ and $\theta'_k$, are defined in a way most nearly equivalent to the customary usage in applications to diffraction by a set of planes (one of which is represented by the broken line) normal to the translation $b_0$. In the case of the linear array, however, $\theta$ and $\theta'_k$ need not be equal, since the only requirement for diffraction is that radiation through adjacent nodes shall experience a path difference, $BC+CD$, which is a multiple of the wavelength $\lambda$. Consequently, the diffraction condition is readily seen to be the single Laue expression

$$b_0(\sin\theta+\sin\theta'_k)=k\lambda,$$

where $k$ is any positive or negative integer specifying a given diffraction. The diffractions emerge as cones whose common axis is that of the array.

Fig. 2 provides a simple transition from the geometry of Fig. 1 to the concepts involved in the use of reciprocal space for consideration of the diffraction of the array. Symbols repeated from Fig. 1 have the same significance. The circle represents the sphere of unit radius, $CO$, commonly designated as the sphere of reflection. $QCP$ is a typical conical diffraction of the array, $P$ and $Q$ being on the sphere. $O$ is the origin of reciprocal space, and the axis $Oy^*$ is parallel to the axis of the array $Cy$. The plane $QPR$, normal to $Oy^*$, is to represent the $k$th diffraction in reciprocal space. Since $OR=OF+EP$, and the last two distances are, respectively, $\sin\theta$ and $\sin\theta'_k$, it follows from the diffraction condition given above that $OR=k\lambda/b_0$. The array will be appropriately represented by a set of parallel planes in reciprocal space, normal to $Oy^*$ with separation $\lambda/b_0$.

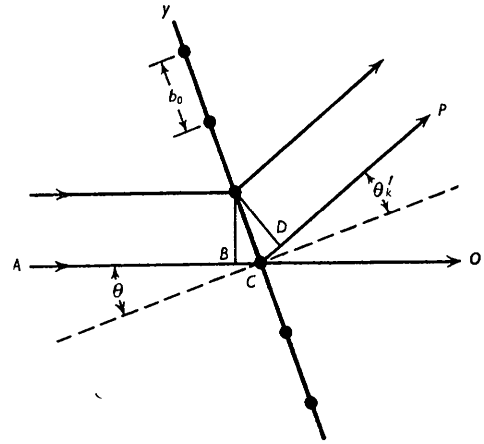


Fig. 1. Illustrating diffraction by a linear array of equivalent nodes spaced $b_0$ apart.

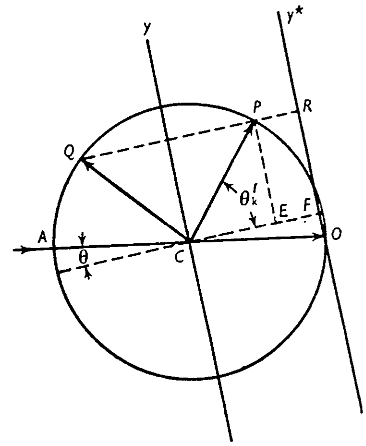


Fig. 2. The reciprocal-space concept applied to a one-dimensional diffractor.

The converse of this, namely, that a set of diffracting planes of separation $b_0$ may be represented in reciprocal space by an array of points, orthogonal to the planes and of separation $b_0$, is the more familiar proposition encountered in crystallography. Since there is no need to postulate structure transverse to $b_0$ in the diffracting planes, both of the above two propositions apply to extreme cases of one-dimensional order. The linear array of nodes is an example with extreme *thinness* transverse to the axis of order, and the set of structureless planes possesses extreme *thickness* transverse to order.

A process may be imagined in which the nodes of the diffracting array are continuously drawn out in space normal to the internodal axis to produce structures intermediate between these two extremes.

During the continuous nodal *expansion* thus imagined the reciprocal-space planes *shrink* through disk-like stages, becoming finally spot-like concentrations when the diffracting nodes become infinite planes. This simple conceptual process discloses qualitatively that the general representation in reciprocal space for a one-dimensionally ordered system may be described as a set of 'disks'. Not only is the separation between the disks ($\lambda/b_0$) reciprocal to the spacing of the diffracting system ($b_0$), but their diameters are reciprocal to dimensions of the diffracting system transverse to order. Disk thickness (along $Oy^*$) depends on the number of internode segments constituting the axial length of the diffracting system, the disks being thinnest when the length of the system is greatest.

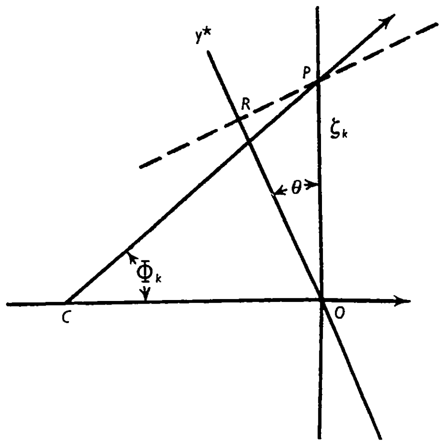


Fig. 3. Use of the 'plane of reflection' at small diffraction angles.

The following additional properties of disks seem fairly obvious from general conceptions regarding diffraction phenomena. If the nodal expansion process described above is carried out so that rotational symmetry is maintained about the axis of the diffracting array, and so that all diameters of the resulting cylinder are equal, all of the reciprocal-array disks will have equal diameters which are therefore independent of index, $k$. Small random fluctuations of internodal separations ($b_0$) result in diminishing the effective coherent length of the diffracting system scattering to each disk; disks of highest absolute $k$ are affected most profoundly, so that disk *thicknesses* increase with $k$. Small random columnar displacements (along axial directions) of material placed at transverse locations in the diffracting system, without disturbance of the $b_0$ periodicity within each column, reduce the effective diameters of the system for coherent diffraction; again disks of largest absolute $k$ are most influenced, so that disk *diameters* increase with $k$.

At small diffraction angles $\lambda$ is much smaller than $b_0$ and the reciprocal-space disks for reasonable values of $k$ lie close to $O$. The sphere of reflection becomes essentially a *plane of reflection* through $O$ normal to the incident beam. Fig. 3 represents the simplified small-angle case, although the diffraction angle, $\Phi_k=\theta+\theta'_k$, is somewhat exaggerated. The vertical line $OP$ now indicates the section of the sphere of reflection near $O$. Because of the unit value of $CO$, positions in the plane of reflection give directly the Bernal co-ordinates $\zeta$ and $\xi$ measuring the vertical and horizontal angular components (the axis for the latter extending normal to the figure plane) of any direction along which diffraction is sent to a registering film. Note that the angle $ROP$ now equals the previously defined $\theta$ (see Fig. 2), which may be termed the angle of tilt, since it measures the departure from the usual perpendicular incidence of the incident X-ray beam upon the axis of the diffracting system.

The $k$th reciprocal-space disk intersects the figure along $RP$ normal to $Oy^*$ at $OR=k\lambda/b_0$. It follows that the vertical angular component of the $k$th disk, $\zeta_k$, is

$$\zeta_k=k\lambda/b_0\cos\theta, \tag{1}$$

which defines a set of observable parallel layer lines in the plane of reflection normal to its meridional ($\zeta$) axis.

Two ways of exploring the reciprocal-space disks are available: With a highly collimated incident beam, perpendicular incidence ($\theta=0$) yields on the diffraction pattern a view of sections through the center of the disks taken parallel with the $\xi$ axis. Variations of $\theta$ accomplished by tilting the specimen for successive photographs yield, at the pattern meridians, successive views of disk locations in the plane of incidence (that of all previous figures). In this way mutually orthogonal sections through each disk may be viewed. However, because of the rotational randomness generally encountered with the fibrillar elements of a fiber, whose common axial direction is the only one controllable with respect to orientation, both experimental approaches furnish equivalent results concerning rotationally averaged disks.

A theoretical, but rarely practical, limitation to the above procedure would be encountered with diffracting systems whose diameters transverse to order are very large. In these cases the structure is essentially a single set of Bragg planes, which should diffract only when $\theta=k\lambda/2b_0$, which is the simplified Bragg law at small angles. This difficulty arises because the reciprocal-space disks are then so restricted in diameter that the curvature of the sphere of reflection cannot be neglected.

Otherwise, the restrictions placed upon equation (1) demand only that $\Phi_k$ be small and not that $\theta$ or $\theta'_k$ be also small separately. Accordingly, when the diffracting structures are of sufficiently small thickness transverse to order, the present approximations are valid at much larger angles of tilt than the Bragg angles corresponding to the spacings involved.

## Nets and lattices

Knowledge of the properties of the disk-like representations of one-dimensional diffracting systems is of importance in studying objects possessing even higher order, since in such cases the structure can be considered as composed of two or three sets of linear arrays. Each of the two sets of linear nodal arrays comprising a two-dimensional net, and corresponding to the two directions of extension in the plane of the net, may be represented in reciprocal space by a set of planes as shown in the last section. It follows that the parallel linear intersections ('rods' below) of the two reciprocal-plane sets constitute the reciprocal-space representation of the actual two-dimensional net, as shown in Fig. 4.

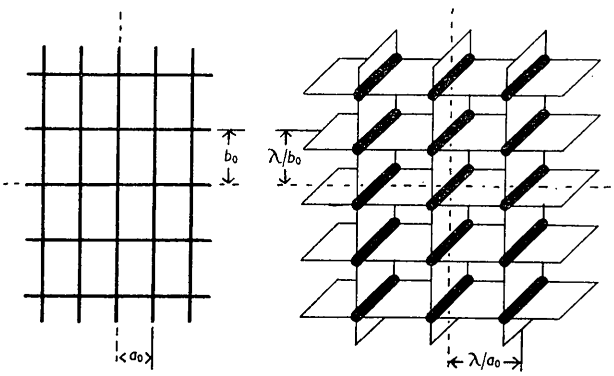


Fig. 4. Comparison of a diffracting net (*a*) with its reciprocal space representation (*b*), which consists of a net of 'rods'.

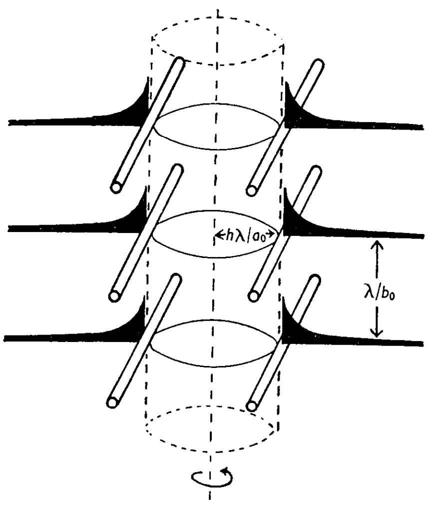


Fig. 5. The inner limiting cylinder produced by rotation of the rods of a net row-line specified by *h*. The solid areas represent sections through the doughnut-like layers produced in reciprocal space by rotation of individual rods, with ordinates indicating density (intensity) at corresponding radial positions in the layers.

Diffraction occurs whenever the reciprocal-space rods cross the plane of reflection. It is impossible, however, with fibrous systems to observe these simple intersections, since the diffraction diagrams obtained are essentially the result of rotating the ultramicroscopic diffracting elements around the *y* or fiber axis. As shown in Fig. 5, because of this rotation, all reciprocal-space rods of constant absolute *h* will form a cylinder of radius $h\lambda/a_0$, from which these rods are excluded during the rotation and which may be called the inner *limiting cylinder*.

Fig. 6 depicts one such cylinder in relation to the plane of reflection at angle of tilt $\theta$. Intersection of cylinder and plane occurs at a *limiting ellipse* whose equation is $\xi^2+\zeta^2\sin^2\theta=(h\lambda/a_0)^2$. Layer lines meet the ellipse at $\zeta_k$ values given by equation (1), so that the relation

$$\xi_{hk}^2=\left(\frac{h\lambda}{a_0}\right)^2-\left(\frac{k\lambda\tan\theta}{b_0}\right)^2 \qquad (2)$$

indicates the $\xi$ co-ordinate of the *h*th ellipse at the level of the *k*th layer line.

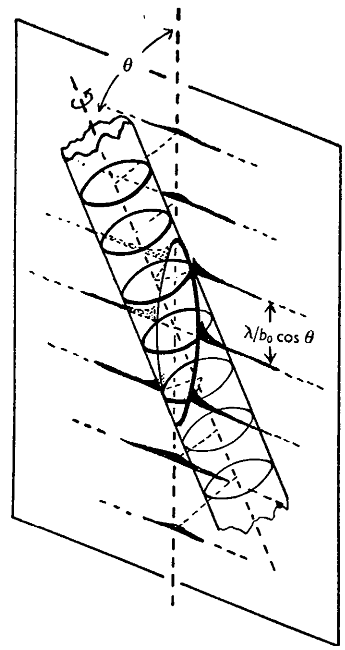


Fig. 6. When the axis of the limiting cylinder (Fig. 5) is tilted out of the plane of reflection, cylinder and plane intersect to form an ellipse, around which diffraction discontinuities must remain until collapsed to the meridian by sufficient tilting.

As uniform rotation occurs, the reciprocal-space rods linger longest in the plane of reflection at positions distributed next to the ellipse. Consequently, equations (1) and (2) define positions corresponding to the most intense diffraction. Along each layer line, and even on layer lines beyond those intersecting a row-line ellipse, diffracted intensity falls off rapidly in directions away from the meridional line. The general description of the asymmetric (*hk*) diffraction is that of extension along the *k*th layer line with rapid fall in intensity away from the maximum value at the abrupt *h*th row-line discontinuities which face toward the meridian (see Fig. 5). In reciprocal space the rotation produces from each rod a doughnut-like averaged layer with a central hole.

Examination of equations (1) and (2) shows that with tilting (increase in $\theta$) the layer lines are displaced, while the row-like discontinuities collapse toward the meridian. At tilts beyond those required to collapse a row-line discontinuity completely to the meridian, the diffraction should still be observed and its position should follow equation (1). According to equation (2), the critical angle of tilt, $\theta_c$, required to complete the collapse ($\xi_{hk}=0$) can be calculated from

$$\tan\theta_c = hb_0/ka_0. \quad (3)$$

When an additional $z$ axis, along which there is now also periodic repetition of structure, is added to those of the two-dimensional net one arrives at the familiar three-dimensional lattice whose representation in reciprocal space is the usual reciprocal lattice, which is composed of points. It is still possible, however, upon tilting the fiber or rotation axis to produce displacements of layer lines and the positions of individual spots on the layer lines.

The derivation of equations dictating the positions of diffraction spots proceeds much as in the two-dimensional case following Fig. 6. The rotation-diagram coordinates, $\xi_{hkl}$, for the spots on a row-line ellipse are given by

$$\xi^2_{hkl} = \frac{\lambda^2}{\sin^2\beta}\left[\left(\frac{h}{a_0}\right)^2 + \left(\frac{l}{c_0}\right)^2 - \frac{2hl\cos\beta}{a_0c_0}\right] - \left(\frac{k\lambda\tan\theta}{b_0}\right)^2, \quad (4)$$

with equation (1) still valid for the layer-line coordinates. As before, the diffraction ($hkl$) moves toward the meridian during tilting to reach it at a critical tilt, $\theta_c$, calculated from

$$\tan\theta_c = \frac{b_0}{k\sin\beta}\left[\left(\frac{h}{a_0}\right)^2 + \left(\frac{l}{c_0}\right)^2 - \frac{2hl\cos\beta}{a_0c_0}\right]^{\frac{1}{2}}. \quad (5)$$

While there is a similarity between equations (2) and (3) of the two-dimensional case, and (4) and (5) of the three-dimensional lattice, the former prescribe positions and critical tilts for the most intense diffraction effects, and the latter indicate rigidly limited conditions for all diffraction. It may be noted also that, according to equation (5), meridional diffractions ($0k0$) should vanish for the slightest tilt (more accurately, for tilts departing from $\theta = k\lambda/2b_0 0$; cf. the remarks above regarding limitation of equation (1) caused by neglecting the curvature of the sphere of reflection).

Indeed, the most readily recognizable diffraction phenomenon accompanying reduction of ordered dimensions below three is that of the persistence with displacement exhibited by each diffraction at tilts above its critical angle $\theta_c$. The critical tilts can be calculated without prior knowledge of the number of ordered axes or before unequivocal indices or lattice dimensions have been established. Both equations (3) and (5) reduce to

$$\tan\theta_c = \xi_0/\zeta_0, \quad (6)$$

where $\xi_0$ and $\zeta_0$ are the angular components observed for the position of maximum intensity of a given diffraction *at zero tilt*. Equation (6) is valid for one-dimensional systems also in the sense that for all reciprocal-array disks $\xi_0 = 0$.

Several qualifications must be added to the preceding paragraphs. The theory for the net neglected the influence of the thickness of the net in the non-ordered direction orthogonal to the plane of the net, and in both net and lattice the diffraction broadening possibly caused by limited extension or any manner of distortion along axes of order was not considered. In examining these situations, the general principles governing reciprocal-array disk diameters and thicknesses will be fundamental in determining the volumes of reciprocal space over which the rod-like or spot-like intersections of the component reciprocal-array disks of the reciprocal net and lattice can extend. In particular, note that the *thickness* of a diffracting net in the non-ordered direction *orthogonal* to the plane of the net determines the *lengths* of the reciprocal-net rods reciprocally.

An unfortunate result of these qualifications to the theory of unlimited ideal nets and lattices is that finite or distorted systems can, on occasion, simulate the diffraction broadening, or the equivalent relaxation of conditions governing angles of beam incidence, shown above to be characteristic of order-deficient systems. This is well known to occur when particle sizes of ordered structures are small. On the other hand, systems with axes lacking order may have extensions of these non-ordered dimensions sufficient to sharpen the diffraction effects. With detailed data regarding line shapes available these various influences might not be confused, but at small diffraction angles they can become difficult to distinguish.

### Criteria for examination of order deficiency

It becomes possible on the basis of arguments given above to enumerate the following particulars which are useful in the determination of the type of order possessed by the ultramicroscopic elements of a fibrous system from its diffraction effects at small angles:

(1) *Resolution*. Because of the importance of the diffraction (layer-line and row-line) structure, it is necessary that the diffraction camera be one capable of resolving all diffractions. The problems of camera construction to insure adequate resolution are considered elsewhere (Bolduan & Bear, 1949).

(2) *Diffraction shapes*. Truly meridional diffractions ($h$ and $l$ zero) will have greatest intensity directly on the pattern meridian, falling off abruptly along layer lines for three-dimensional order but less precipitously for lesser degrees of order. Other diffractions ($h$ and $l$ not both zero) will be simple and sharp for three-dimensional order; asymmetric for two-dimensional order (see Fig. 5); and non-existent for one-dimensional order.

(3) *Diffraction displacement with tilt*. In all cases the layer lines change in position with tilt according to equation (1). However, only with diffractions of one- and two-dimensional systems can this equation normally be followed experimentally much beyond the critical tilts given by such equations as (3) and (5), or more generally by equation (6). Meridional diffractions

are particularly useful, since with them practically the entire range of tilting is applicable to the demonstration of order deficiency.

(4) *Fibril orientation.* In examples whose diffracting elements (fibrils) are not all perfectly aligned with the fiber axis, true diffraction shapes may be difficult to observe and the diffractions may also persist for appreciable tilts beyond those permitted for three-dimensional systems, solely because of poor orientation. To determine that this persistence is spurious, and not related to possession of lesser order, it is sufficient to note that the layer lines *do not move* as a function of tilt strictly according to equation (1). Also, at zero tilt it will be seen that the individual diffractions are arcs of circles and not spread out straight along the layer lines.

(5) *Fibril thickness.* The fibrils are generally so long in terms of $b_0$ translations that layer lines are extremely sharp, and the major part of an investigation becomes concerned with the shapes and positions of the individual diffractions as these may be spread upon the layer lines. One may conclude that this spreading, or the equivalent persistence with tilt, is direct evidence for a deficiency in axes of order only if there is reason to believe that any possible ordered transverse dimensions are sufficiently large to prevent the similar spreading which accompanies limited extension of order. Conversely, the spreading evidences for axes lacking order may be absent when the non-ordered dimensions are large. Consequently, the only unequivocal demonstration of the number of axes of order depends on the number of lattice translations in evidence, but when less than three of these are readily apparent it is reassuring to be able to secure additional evidence by showing that the appropriate line spreading and tilt phenomena exist.

(6) *Distortion.* The criteria given to this point are applied most simply to diffracting structures whose extension in ordered and non-ordered directions may be said to be perfect. One frequently encounters imperfect systems, whose effective coherently scattering dimensions are less than the actual fibril dimensions because of internal distortions of structure. The most general way to recognize the nature of these imperfections is that of studying variations of observed spot or line dimensions, or persistence with tilt, as functions of diffraction indices. General knowledge of how various types of imperfection influence dimensions of reciprocal-space disks, rods, or points then facilitates interpretation of the data. Examples drawn from protein fibers will be given elsewhere.

(7) *Symmetry of diffraction patterns.* Because of the inherent centrosymmetry of reciprocal space and the rotational symmetry introduced by the random rotational orientation of fibrils about a fiber axis, fiber diagrams obtained *at zero tilt* should be symmetrical about meridional and equatorial lines. *Tilting*, however, should destroy the pattern symmetry relative to the equatorial line if the curvature of the sphere of reflection is not negligible compared with the dimensions of the disks, rods and points of reciprocal space. Indeed, observation of the production of this type of pattern asymmetry provides a sensitive test as to whether the sphere of reflection may be regarded as a plane of reflection at small diffraction angles. Because this simplification is usually possible most fiber patterns at small angles remain symmetrical relative to the equatorial line even after considerable tilting of the specimen.

## References


Bear, R. S. (1944*a*). *J. Amer. Chem. Soc.* **66**, 1297.

Bear, R. S. (1944*b*). *J. Amer. Chem. Soc.* **66**, 2043.

Bear, R. S. (1945). *J. Amer. Chem. Soc.* **67**, 1625.

Biscoe, J. & Warren, B. E. (1942). *J. Appl. Phys.* **13**, 364.

Bolduan, O. E. A. & Bear, R. S. (1949). *J. Appl. Phys.* **20**, 983.

Ewald, P. P. (1940). *Proc. Phys. Soc. Lond.* **52**, 167.

Hall, C. E., Jakus, M. A. & Schmitt, F. O. (1945). *J. Appl. Phys.* **16**, 459.

James, R. W. (1948). *The Optical Principles of the Diffraction of X-rays.* London: Bell.

Nowacki, W. (1946). *Schweiz. ChemZtg.* Nr. 14–15.

Schmitt, F. O., Hall, C. E. & Jakus, M. A. (1942). *J. Cell. Comp. Physiol.* **20**, 11.

Warren, B. E. (1941). *Phys. Rev.* **59**, 693.

West, C. D. (1947). *J. Chem. Phys.* **15**, 689.